



Short-range axono-cortical evoked-potentials in brain tumor surgery: Waveform characteristics as markers of direct connectivity

Olivier Rossel, Félix Schlosser-Perrin, Hugues Duffau, Riki Masumoto, Emmanuel Mandonnet, François Bonnetblanc

► To cite this version:

Olivier Rossel, Félix Schlosser-Perrin, Hugues Duffau, Riki Masumoto, Emmanuel Mandonnet, et al.. Short-range axono-cortical evoked-potentials in brain tumor surgery: Waveform characteristics as markers of direct connectivity. *Clinical Neurophysiology*, 2023, 48 (8), pp.550-554. 10.1016/j.clinph.2023.05.011 . hal-04135237

HAL Id: hal-04135237

<https://inria.hal.science/hal-04135237>

Submitted on 20 Jun 2023

HAL is a multi-disciplinary open access archive for the deposit and dissemination of scientific research documents, whether they are published or not. The documents may come from teaching and research institutions in France or abroad, or from public or private research centers.

L'archive ouverte pluridisciplinaire **HAL**, est destinée au dépôt et à la diffusion de documents scientifiques de niveau recherche, publiés ou non, émanant des établissements d'enseignement et de recherche français ou étrangers, des laboratoires publics ou privés.



Distributed under a Creative Commons Attribution 4.0 International License

Short-range axono-cortical evoked-potentials in brain tumor surgery: waveform characteristics as markers of direct connectivity

Olivier Rossel¹, Félix Schlosser-Perrin¹, Hugues Duffau², Riki matsumoto³, Emmanuel mandonnet^{4,+}, François Bonnetblanc^{1,+,*}

¹ CAMIN Team, INRIA, Université de Montpellier, France

² Département de Neurochirurgie, Centre Hospitalier Universitaire de Montpellier Gui de Chauliac, Montpellier, France

³ Division of Neurology, Kobe University Graduate School of Medicine, Japan

⁴ Département de Neurochirurgie, Centre Hospitalier Universitaire, Hôpital Lariboisière, Paris, France

+ Both authors supervised this work.

* Corresponding author: francois.bonnetblanc@inria.fr

Abstract

Objective: Intraoperative measurement of axono-cortical evoked potentials (ACEP) has emerged as a promising tool for studying neural connectivity. However, it is often difficult to determine if the activity recorded by cortical grids is generated by stimulated tracts or by spurious phenomena. This study aimed to identify criteria that would indicate a direct neurophysiological connection between a recording contact and a stimulated pathway.

Methods: Electrical stimulation was applied to white matter fascicles within the resection cavity, while the evoked response was recorded at the cortical level in seven patients.

Results: By analyzing the ACEP recordings, we identified a main epicenter characterized by a very early positive (or negative) evoked response occurring just after the stimulation artifact (< 5 ms, $|\text{Amplitude}| > 100 \mu\text{V}$) followed by an early and large negative (or positive) monophasic evoked response (< 40 ms; $|\text{Amplitude}| > 300 \mu\text{V}$). The neighboring activity had a different waveform and was attenuated compared to the hot-spot activity.

Conclusions: It is possible to distinguish the hotspot with direct connectivity to the stimulated site from neighboring activity using the identified criteria.

Significance: The electrogenesis of the ACEP at the hotspot and neighboring activity is discussed.

Keywords: Direct Electrical Stimulation · Evoked Potentials · Electrocorticography · Axono-Cortical Evoked Potential · Awake Brain Surgery · Tumors · Intra-Operative Neural Monitoring.

Abbreviations

AP: Action Potentials; ACEP: Axono-Cortical Evoked Potentials; CD: Contact Diameter; DES: Direct Electrical Stimulation; DCR: Direct Cortical Response; CCEP: Cortico-Cortical Evoked Potential; EP: Evoked Potentials; EPSP: Excitatory Post Synaptic Potentials; FAT: Frontal Aslant Tract; IFOF: Inferior Fronto-Occipital Fasciculus; ECoG: ElectroCorticography.

1. Introduction

Direct electrical stimulation (DES) is a valuable tool used during brain tumor resection surgeries to identify critical cortical and subcortical areas for function. It induces transient behavioral and cognitive disturbances, facilitating the mapping of essential cortical areas and white matter pathways (Duffau, 2015; Mandonnet et al., 2010). Despite its widespread use, the electrophysiological effects of DES remain poorly understood, primarily due to the significant methodological variations between protocols (Boyer et al., 2021a; Vincent et al., 2017, 2016). To gain a better understanding of DES's electrophysiological effects, evoked potential (EP) recordings are used to study the conductive and integrative properties of neural assemblies and brain connectivity (Boyer et al., 2021a, 2020, 2018; Matsumoto et al., 2006, 2004; Vincent et al., 2020).

In 1936, Sir Edgar Douglas Adrian first described a surface negative potential that followed a brief electrical stimulus applied to the cerebral cortex's surface. This observation and subsequent works, especially in the 1950s and 60s, were essential in understanding electrical brain activity's spread. This "Direct Cortical Response" or DCR (Goldring et al., 1961) was initially attributed to direct excitation of dendrites in the superficial layers only (Adrian, 1936). Further studies, using additional unitary extracellular recordings, suggested that these classical surface negative potentials might represent excitatory postsynaptic potentials set up in apical dendrites (Eccles, 1951; Li and Chou, 1962). The depolarization or synaptic potentials of recorded extracellular spikes were found to be linearly proportional to the surface negative potential (Li and Chou, 1962). With increasing stimulus strength, this early negative response was followed by a smooth surface positive wave or a second surface negative large peak (Adrian, 1936; Chang, 1951; Li and Chou, 1962, see Figure 2). These later components were thought to represent evoked activity of cell body and dendrites of pyramidal neurons in the deeper layers of the cortex (Adrian, 1936; Chang, 1951; Li and Chou, 1962), or inhibitory activities (Usami et al. 2015).

In the neurosurgical context, DCR is one of three types of cortical potentials (EP) evoked by electrical stimulation applied to the brain. It can be measured in the immediate vicinity (same gyrus) of the cortical stimulation site. The other two are true cortico-cortical evoked potentials (CCEP), recorded remotely from the stimulation site, and axono-cortical potentials (ACEP), evoked cortically after subcortical stimulation of white matter pathways (Boyer et al., 2021b, 2021a; Mandonnet et al., 2016; Vincent et al., 2017, 2020; Wasserman et al., 2021). Recording CCEP and ACEP is more challenging because these EP are necessarily attenuated and delayed in time compared to DCR evoked at the stimulation site due to the electrophysiological propagation of the response through white matter pathways. The divergence in their termination induces a reduced spatiotemporal summation of electrophysiological events remotely (Matsumoto et al., 2004, 2007; Yamao et al., 2014; Enatsu et al., 2013, 2016; Boyer et al., 2018, 2020; Boyer et al., 2021a).

In this context, the electrogenesis of cortico-cortical evoked potentials (CCEP) and axono-cortical evoked potentials (ACEP) is not yet well established and their heterogeneity remains to be fully elucidated and understood (Boyer et al., 2021b, 2021a; Matsumoto et al., 2006, 2004; Miller et al., 2021). However, these evoked potentials, particularly ACEP, hold potential for online connectivity probing and identification of critical fascicles during surgery, as well as improved understanding of the electrophysiological effects of DES in the human brain. Therefore, efforts towards a taxonomy of brain evoked potentials with accurate

identification, characterization, and interpretation of ACEP are essential to achieve these goals. Specifically, identifying a prototypic waveform that can serve as a biomarker of the highest connectivity to the stimulation site is crucial from both neuroscience and neurosurgical perspectives.

Here, we present our experience with intraoperative ACEP recordings in seven patients. In each case, different white matter fascicles were identified as functional boundaries of the resection and were stimulated at either 1 or 9 Hz, while electrode strips were placed over various cortical regions surrounding the cavity.

2. Methods

A total of seven patients underwent awake brain surgery, with five patients (1, 3, 4, 6 and 7) operated on in Paris by one neurosurgeon (EM) and two patients operated on in Montpellier (2 and 5) by another neurosurgeon (HD). The study, UF 965, n° 2014 A00056 43, was approved by the local ethics committee.

2.1. Anesthetic protocols

The anesthetic protocols used for each patient depended on the location of their surgery. In Paris, the full awake technique was used as previously reported (Aubrun et al., 2020). This involved monitored anesthesia care to achieve sedation while preserving spontaneous ventilation without any airway instrumentation. Sedation was achieved using a combination of propofol, remifentanyl, and dexmedetomidine, and was completely stopped during the awake phase.

In Montpellier, a different protocol was followed based on the study "Intermittent general anesthesia with controlled ventilation for asleep awake asleep brain surgery" (Deras et al., 2012). Briefly, general anesthesia was induced by intravenous infusion of DIPRIVAN® (propofol) and Remifentanyl, which are short-acting medications and opioid analgesic drugs, respectively, that have a rapid onset and recovery time. When a laryngeal mask airway was used, the target concentration for propofol was 6 mg ml⁻¹ and 6 ng ml⁻¹ for Remifentanyl. When tracheal intubation was preferred, the targets were 12 mg ml⁻¹ and 12 ng ml⁻¹, respectively.

2.2. Intraoperative functional mapping

Standard cortical and white matter mapping were performed on all awake patients. Intraoperative functional mapping was carried out using 60 Hz direct electrical stimulation (DES) while patients performed cognitive and motor tasks. Functional sites identified during the operation were tagged with numbered labels placed on the brain surface. A manual bipolar probe was used to deliver an adjustable biphasic current square wave pulse with the Nimbus i care (Innopsys, Toulouse, France) at frequencies of 60 Hz. The intensity was set between 1.5 and 5 mA, with a single pulse duration of 0.5 to 1 ms. The intensity was increased in steps of 0.5 mA until the stimulation elicited a clinical response, but without inducing seizures. DES was performed on the entire exposed area, with the probe being displaced every 5 mm in two orthogonal directions. The duration of the effective stimulation was determined based on the mapped function, with 1 s used to induce positive motor and sensory responses and up to 4 s used to inhibit cognitive ones. Several stimulation conditions were tested and repeated twice consecutively at each stimulation site. If a functional disturbance was consistently induced, the surgeon avoided resecting the stimulated area. The 60 Hz intraoperative functional mapping for each patient is summarized in Table 1, and the locations of functional sites are labeled on Figures 1-7.

Table 1. Summary of the intraoperative functional mapping.

Patient	<ul style="list-style-type: none"> Gender, Age, Laterality, Volume of the Tumor, Nature of the Tumor, Location Cortical 60Hz DES Intra-operative mapping: <ul style="list-style-type: none"> Label, site location: behaviorial effect (DES intensity, Pulse Duration) Subcortical 60Hz DES Intra-operative mapping: <ul style="list-style-type: none"> Label, site location: behaviorial effect (DES intensity, Pulse Duration)
1	<ul style="list-style-type: none"> Female, 38, Left, 4 cm3, cavernome, right parietal operculum. Cortical mapping: <ul style="list-style-type: none"> 1, ventral premotor cortex: speech arrest during picture naming but not during counting (2.7 mA, 0.5 ms) 2-3, post-central gyrus: tingling in the thumb and in the mouth (2.5 mA, 0.5 ms) Subcortical mapping: <ul style="list-style-type: none"> 10, pre-central operculum: complete motor arrest (3 mA, 0.5 ms)
2	<ul style="list-style-type: none"> Male, 36, Right, 5.8 cm3, diffuse low grade glioma, left, inferior frontal gyrus Cortical mapping: <ul style="list-style-type: none"> 1, ventral premotor cortex: lateral part of the precentral gyrus: movement of the right upper limb and counting arrest (2.5 mA, 1 ms) 2, ventral premotor cortex: retro central part of the Rolandic operculum: dysarthric problem linked to dysesthesia at the level of the tongue (2.5 mA, 1 ms) 3, dorsolateral prefrontal cortex: two episodes of semantic disorders during the PPTT test (2.5 mA, 1 ms) Subcortical mapping: <ul style="list-style-type: none"> 49, Frontal Aslant Tract (FAT): arrest of the fluency (2.5 mA, 1 ms) 50, Inferior Fronto-Occipital Fascicle (IFOF): semantic paraphasias (2.5 mA, 1 ms)
3	<ul style="list-style-type: none"> Female, 30, Right, 30 cm3, diffuse low-grade glioma, right, pars opercularis of the precentral gyrus Cortical mapping: <ul style="list-style-type: none"> 1, post-central gyrus: tingling in the thumb (1.75 mA, 0.5 ms) 2, post-central gyrus: tingling in the mouth on the left side (2 mA, 0.5 ms) 3, pre-central gyrus: stoping of the counting task but not of the repetitive movements of the arm 4, pars opercularis: errors on the 3-digit forward digital span (2.75 mA, 0.5 ms) 5, very anterior part of the supramarginal gyrus: errors on the 3-digit forward digital span (2.75 mA, 0.5 ms) Subcortical mapping: <ul style="list-style-type: none"> 8, mesial face of the parietal operculum: sensation of heat in the head and the left arm (2.75 mA, 0.5 ms) 9, mesial face of the parietal operculum: vibrations in the tongue, a little higher (2.75 mA, 0.5 ms) 6, 10 white matter of the precentral gyrus: movements of the mouth (2.75 mA, 0.5 ms) 11, third branch of the superior longitudinal fasciculus (SLF): errors in the forward 3 digits span, and even more frequent errors in the backward 3 digits span (2.75 mA, 0.5 ms)
4	<ul style="list-style-type: none"> Male, 31, Right, 25 cm3, diffuse low-grade glioma, right temporo-parietal junction Cortical mapping: <ul style="list-style-type: none"> 1, post-central gyrus: tingling in the ring finger (2.25 mA, 0.5 ms) Subcortical mapping: <ul style="list-style-type: none"> 7, fundus of the intra parietal sulcus: attentional dropout and deviation to the right at the line bisection (4 mA, 0.5 ms) 2,3 and 4, temporal termination of the inner branch of the arcuate fasciculus: disturbance of the forward or backward digit span (3 mA, 0.5 ms) 5, deep parietal operculum at its mesial face just above the insular surface: sensation of warmth in the left side (3 mA, 0.5 ms) 6, deep parietal operculum at its mesial face just above the insular surface: sensation of warmth also accompanied by vibrations (3 mA, 0.5 ms) 7, depth of the post central sulcus: sensation of vibration associated with tingling rather in the left upper body (3 mA, 0.5 ms)
5	<ul style="list-style-type: none"> Female, 31, Right, 21 cm3, diffuse low-glioma, left, junction between the pre-central gyrus and the pre-motor region. Cortical mapping: <ul style="list-style-type: none"> 1-2-3-4 and 5, ventral premotor cortex: complete anarthria (2.5 mA, 1 ms) 11, lateral part of the precentral gyrus: suspension of both fluency and movement of the right upper limb (2.5 mA, 1 ms) 7-8 and 9, primary motor area of the face: posterior part of the pre-central gyrus: involuntary facial movements (2.5 mA, 1 ms) 12, precengral gyrus: systematically inducing anarthria more or less associated with an arrest of movement of the right upper limb (2.5 mA, 1 ms) 10, precentral gyrus: knob of the hand, involuntary dystonic movements (2.5 mA, 1 ms) 13, dorso-lateral pre-frontal cortex: semantic disorders during the PPTT test (2.5 mA, 1 ms) Subcortical mapping: <ul style="list-style-type: none"> 14, anterior part of the IFOF as well as of the FAT: complete anomia (2.5 mA, 1 ms) 49, underneath the dorso lateral pre-frontal cortex: junction between the oculo-motor and the fronto-striatal fascicles: an arrest of the movement of the right upper limb with involuntary ocular saccades (2.5 mA, 1 ms) 50, FAT: stuttering (2.5 mA, 1 ms) 46, anterior part of the arcuate fascicle: phonological paraphasias (2.5 mA, 1 ms) 48, junction pyramidal fibers which come from the primary laryngeal motor area and FAT: anarthria and vocalizations (2.5 mA, 1 ms) 47, corticospinal fibers which come from the primary motor area of the face: articulatory disorders with involuntary facial movements (2.5 mA, 1 ms)
6	<ul style="list-style-type: none"> Male, 35, right, 90 cm3, diffuse low-grade glioma, left, middle frontal gyrus. Cortical mapping: <ul style="list-style-type: none"> 1-2-3, postcentral gyrus: fingers movement (1.7 mA, 0.5 ms) 4, post-central gyrus: tingling in the tongue (1.7 mA, 0.5 ms) 5, pre-central gyrus: complete motor arrest (2 mA, 0.5 ms) 6, lower end of pre-central gyrus: speech arrest without an arrest of arm movement (1.7 mA, 0.5 ms) 7, pars opercularis: anomia / semantic paraphasia (2 mA, 0.5 ms) 8, posterior part of the superior frontal gyrus: stopping of spontaneous language but not of picture naming (2 mA, 0.5 ms) Subcortical mapping: <ul style="list-style-type: none"> 1, fibers of frontal eye fields: eye movement and absence (3 mA, 0.5 ms) 2, anomia (below the superior frontal sulcus: potentially Aslant fascicle (3 mA, 0.5 ms) 3, junction between Aslant tract and SLF): anomia (3 mA, 0.5 ms) 4, junction between Aslant tract and IFOF): anomia (3 mA, 0.5 ms)
7	<ul style="list-style-type: none"> Male, 57, right, 1,5 cm3, oligodendroglioma, right supra-marginal gyrus. Cortical mapping: <ul style="list-style-type: none"> no functional site was identified (3 mA, 0.5 ms) Subcortical mapping: <ul style="list-style-type: none"> 1, depth of posterior insular point: feeling of electric current in the left leg (2 mA, 0.5 ms) 2, upper part of the optical radiation: phosphenes in the left inferior quadrant (3 mA, 0.5 ms)

DES: Direct Electrical Stimulation; FAT: Frontal Aslant Tract; IFOF: Inferior Fronto-Occipital Fasciculus.

2.3. Post-resection Electrocorticographic (ECoG) recordings

Electrocorticographic (ECoG) recordings were performed in two settings: under general anesthesia in Montpellier and while patients were awake and resting in Paris. Subcortical sites that had been identified as functional areas during the brain mapping were stimulated with low frequency Direct Electrical Stimulation (DES) at 1, 3, or 9 Hz, with pulse duration (PW) of 0.5 or 1 ms. The number of pulses per epoch and time window between pulses were adjusted based on the stimulation frequency to capture early and/or late components of the evoked potentials. ECoG data were recorded after tumor resection using platinum contact strips with a radius of 2.5 mm and 10 mm spacing (DIXI, France) placed on the surface of the brain. ECoG signals were recorded using a referenced (common or monopolar) mode, with a sampling rate of 38.4 kHz (g.HIAMP, G.tec, Austria). Ground and reference electrodes (Medtronic DME 1004) were placed on the acromion and ipsilesional mastoid, respectively.

Multiple channels were measured for each patient, and signals were recorded without filtering. Post-processing involved removing artifacts (replaced by interpolation, during stimulation duration plus the following 4 ms) and 50 Hz noise, and filtering the data between 1 Hz and 1000 Hz. The procedure for identifying and removing the 50 Hz noise involved selecting a channel with higher noise, building an averaged pattern representative of the noise, selecting another channel where the averaged pattern repeated, extracting a second averaged pattern specific to this channel, and subtracting it. This process was repeated for all channels of interest, taking advantage of the synchronous nature of 50 Hz noise across all channels.

Mean traces of evoked potentials were obtained by averaging ECoG signals synchronized to the DES. Each epoch contained between 38 and 86 pulses, depending on the stimulation rate (i.e. $f=1, 3$ or 9 Hz) and duration (varying between 9 to 61s; Patient 1: $f=1$ Hz, $T=61$ s, $n=61$ stimulations. Patient 2: 3 Hz, 14 s, 43; Patient 3: 3 Hz, 27 s, 81; Patient 4: 3 Hz, 19 s, 58; Patient 5: 9 Hz, 9 s, 86; Patient 6: 1 Hz, 38 s, 38; Patient 7: 3 Hz, 23 s, 68). The baseline of each stimulus was defined using the mean value of the 100 last milliseconds preceding each stimulus artifact (except for Patient 5 where the DES frequency was 9Hz: 10 ms were used for rebasing the signals). The stability and repeatability of EPs over time was checked to control for possible adaptation induced by the stimulation frequency.

For ACEP evocation, each subcortical site demonstrating a behavioral effect during the initial 60 Hz intra-operative mapping was stimulated again at low frequency, except for Patients 3 and 7. For Patient 3, DES was applied between a cortical site (4) and a subcortical site (11) in order to follow a pathway linking the two sites. In Patient 7, redo surgery limited the positioning of ECoG strips to the close vicinity of the resection (due to pial adherences), and the DES site was constrained to a location just below an ECoG location that was not a functional site. Only recordings satisfying inclusion criteria were selected (see Table 2).

Table 2. Contingency Table of total subcortical stimulations in the gyral white matter pathways: observed EP, canonical ACEPs, double-positive waveforms, rejected and selected ones with exclusion and inclusion criteria.

Patients	# Subcortical stimulations (sites as reported for Table 1)	# observed EP (sites)	# Canonical ACEPs : i.e. (P0)-N1 or (N0)-P1 waveform (sites)	# Double-positive waveforms (sites)	# Rejected (sites): with exclusion criteria	# Selected (sites): with inclusion criteria
1	1 (10)	1 (10)	1 (10)	1 (10)	0	1 (10): canonical ACEP with P0-N1 or N0-P1 waveform and increased magnitude, showing additional double positive waveform
2	11 (50 and around 50 in order to track the IFOF)	7 (50 and around 50 in order to track the IFOF)	7(50 and around 50 in order to track the IFOF)	1(round 50)	6 (50 and around 50 in order to find the IFOF): extra-gyral white matter pathways, small magnitude and no double-positive waveform	1 (50): canonical ACEP with P0-N1 or N0-P1 waveform and increased magnitude, showing additional double positive waveform
3	3 (11, 6, below cortical site 4)	3 (11, 6, below cortical site 4)	2 (6, below cortical site 4)	1 (below cortical site 4)	1 (6): small magnitude and no double-positive waveform	1 (below cortical site 4): canonical ACEP with P0-N1 or N0-P1 waveform and increased magnitude, showing additional double positive waveform
4	3 (1, 2, 3)	2 (1, 2)	1 (1)	0	1 (2): no double-positive waveform	1 (1): canonical ACEP with P0-N1 or N0-P1 waveform and increased magnitude, showing additional double positive waveform
5	4 (46, 47, 48, 49)	2 (47, 48)	2 (47, 48)	0	2 (47): no double-positive	1 (48): canonical ACEP with P0-N1 or N0-P1 waveform and increased magnitude
6	4 (1, 2, 3, 4)	3 (1, 2, 4)	1 (2)	0	2 (1, 4): no double-positive waveform	1 (2): canonical ACEP with P0-N1 or N0-P1 waveform and increased magnitude
7	2 (<2 cm and >2 cm below cortical site 1)	1 (<2 cm below cortical site 1)	0	1 (<2 cm below cortical site 1)	0	1 (<2 cm below cortical site 1): double positive waveform and quite important magnitude

ACEP: Axono-Cortical Evoked Potentials; EP: Evoked Potentials; IFOF: Inferior Fronto-Occipital Fasciculus.

3. Results: post-resection ECoG recordings of ACEP

The application of DES to subcortical white matter tracts induced two types of ACEPs. The first type consisted of a very early positive (Patients 1-3) or negative (Patient 5) evoked response occurring just after the stimulation artefact (<10 ms), which was followed by an early and large negative (Patients 1-4) or positive (Patient 5) monophasic evoked response (<40 ms; $|\text{Amplitude}| > 300 \mu\text{V}$), immediately followed by an after positivity (or after negativity for Patient 5). The second type of ACEPs had an early and a late component (>75 ms), both positive but with a significantly lower amplitude ($\text{Amplitude} < 200 \mu\text{V}$) (Patients 1, 2, 6, and 7). These observations were reproducible despite varying conditions, as they were observed on both hemispheres (L: Patients 1, 4, and 6 vs. R: Patients 2, 3, 5, and 7), in different anatomical territories (see Table 1), hence different white matter tracts, and for two hospitals with two different surgeons.

For Patient 1, DES applied ($f=1$ Hz, $I=3$ mA, $PW=0.5$ ms) in the anterior wall of the resection cavity (fibers of the operculum converging towards functional site 1) induced different waveforms of ACEP. These included a very early positive 2.6 ms component (Amplitude > 100 μ V) followed by a 14.8 ms and large negative evoked response ($|Amplitude| > 300$ μ V) observed on contact 2 with an immediate small after positivity. An early (17 ms) but attenuated response on contact 1 was suspected to be a remote capture (through passive volume conduction) of the response evoked near contact 2 (as shown in Figure 1 D in which the ACEP in ECoG 1 is equivalent to the ACEP in ECoG 2 up to a scale factor equal to 3). A double positive potential, with an early (8.4 and 19 ms) but attenuated response and a late component (95 ms) whose amplitude was also inferior to 200 μ V, was observed on contacts 3 and 4 (with an attenuation of the late component for this later contact). Interestingly, for contacts 3 and 4, the very early component occurring before 5 ms was not observed.

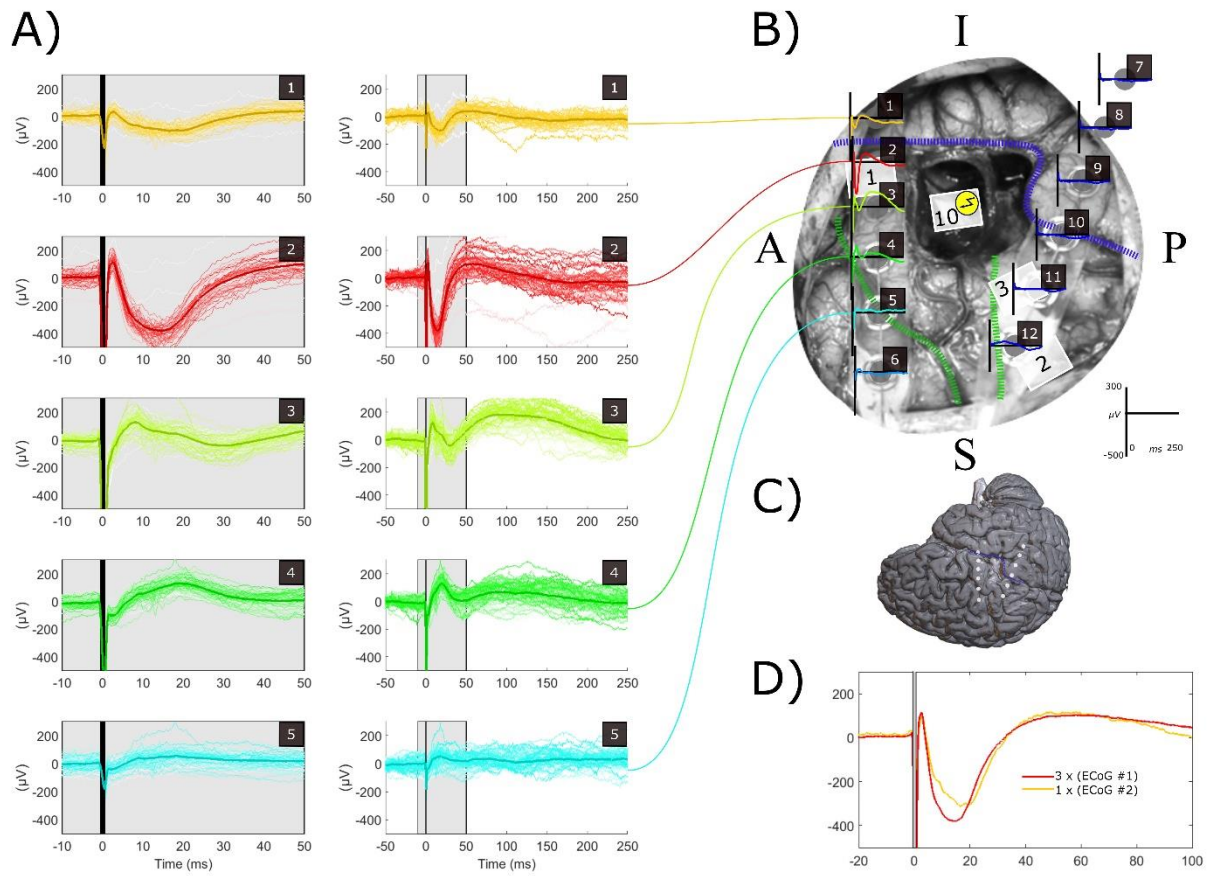


Figure 1. Patient 1: Positioning of ECoG strips (2 x 6 contacts) (B), stimulation sites and ACEP (A and B). The first ECoG strip was centered on the pre-central gyrus. Contact 1 being on the temporal lobe and contact 6 just in front of the precentral sulcus. The second ECoG strip was located on the supramarginal gyrus for contacts 7-10 and the post-central gyrus for contact 11-12 approximately. DES ($f=1$ Hz, $I=3$ mA, $PW=0.5$ ms) was applied subcortically on the opercular white matter, i.e. site 10 (inducing a motor arrest during 60 Hz DES mapping). ACEP show different shape and amplitude. Red indicates earlier and greater negative potentials. Green indicates double positive potentials. Blue stand for absence of evoked responses. A) Left signals in the grey box are zoomed from $[-10$ ms; $+50$ ms] in the right column. The black vertical line covers the whole DES artefact. Main anatomical landmarks were identified by thick dashed-line: Sylvian fissure in blue, central sulcus in light green, precentral sulcus in dark green. B) The broken arrow in the yellow circle represents the subcortical DES site. C) Localization of the craniotomy with ECoG

positioning in the brain in the 3D post-operative Brain. D) Scaling of ECoG 1 to ECoG 2 in order to illustrate the fact it is roughly the same signal capture remotely.

ACEP: Axono-Cortical Evoked Potentials; DES: Direct Electrical Stimulation; ECoG: ElectroCorticography.

For Patient 2, DES applied ($f=3$ Hz, $I=2.5$ mA, $PW=1$ ms) in the resection cavity on the inferior fronto-occipital fasciculus (IFOF) induced different waveforms of ACEP. These included a very early positive 3.7 ms (Amplitude > 100 μ V) component followed by a 19.5 ms and large negative evoked response (|Amplitude| > 300 μ V) observed on contact 16 with an immediate small after positivity. Identical (~ 20 ms: 21, 19, and 20 ms) but attenuated responses were observed on contacts 15, 1, and 2, respectively, which were suspected to be remote captures of the response evoked near contact 16 (as shown in Figure 2 D in which the ACEP in ECoG 1, 2 and 15 are equivalent to the ACEP in ECoG 16 up to a scale factor equal to 1.4, 3.5 and 2.3 respectively). A double positive potential, with an early (12.5 ms) but attenuated response and a late component (around 70 ms) whose amplitude was very attenuated on contacts 7 and 3, was observed. In this patient also, the very early component occurring before 5 ms was not observed for contacts 7 and 3.

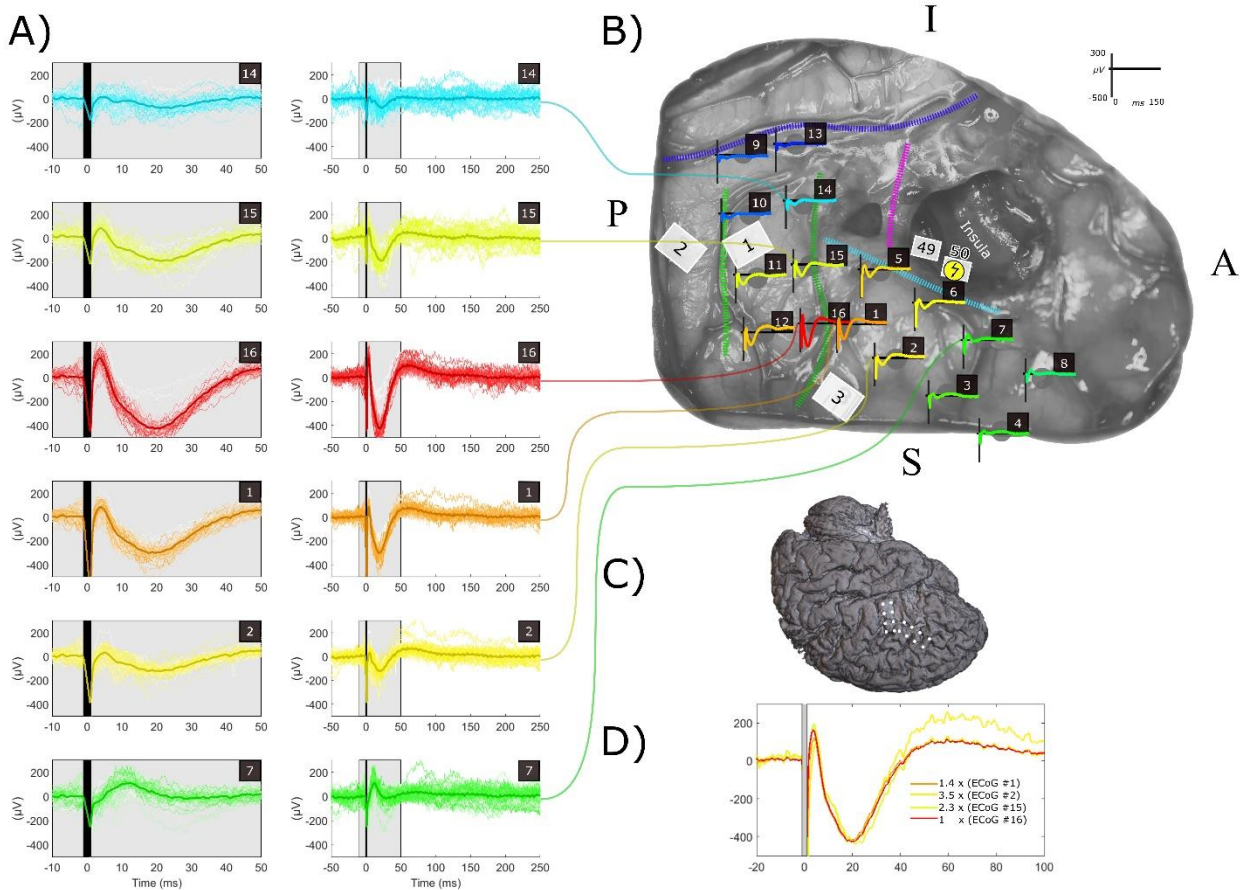


Figure 2. Patient 2: Positioning of ECoG strips (4 x 4 contacts) (B), stimulation sites and ACEP (A and B). 2 x 4 ECoG contacts were placed in parallel in the middle frontal gyrus numbered from 1 to 8 (1 and 5 being in the more posterior part and 4 and 8 being in the more anterior part); (ii) and 2 x 4 others ECoG contacts were also placed together in parallel in the pre-central gyrus numbered from 9 to 16 (9 and 13 being in the ventral part, 12 and 16 in the dorsal part). DES ($f=3$ Hz, $I=2.5$ mA, $PW=1$ ms) was applied subcortically on the white matter pathways on the IFOF, i.e. site 50 (inducing semantic paraphasia during 60 Hz DES mapping). ACEP show different shape and amplitude. Red indicates earlier and greater negative potentials. Green indicates double positive potentials. Blue stand for absence of evoked responses. A) Left signals in the grey box are zoomed from $[-10\text{ms}; +50\text{ms}]$ in the right column. The black vertical line covers the whole DES artefact. B) The broken arrow in the yellow circle represents the subcortical DES site. Main anatomical landmarks were identified by thick dashed-line: Sylvian fissure in blue, central sulcus in light green, precentral sulcus in dark green, inferior frontal sulcus in cyan, ascendant ramus of the sylvian fissure in pink. C)

Localization of the craniotomy with ECoG positioning in the brain in the 3D post-operative Brain. D) Scaling of ECoG 1, 2, 15 to ECoG 16 in order to illustrate the fact it is roughly the same signal capture remotely on these electrodes. ACEP: Axono-Cortical Evoked Potentials; DES: Direct Electrical Stimulation; ECoG: ElectroCorticography; IFOF: Inferior Fronto-Occipital Fasciculus.

For Patient 3 (Figure 3), applying DES ($f=3$ Hz, $I=2.75$ mA, $PW=0.5$ ms) in the white matter of the frontal operculum induced different waveforms of ACEP. On contact 21, a very early positive component (4.9 ms, amplitude > 100 μ V) was followed by a large negative response (22.4 ms, $|\text{amplitude}| \approx 200$ μ V), with an immediate small after-positivity. Identical responses were observed on contacts 19, 20, 22, and 23, but with lower amplitudes (~ 20 ms: 21.1, 21.5, 21.6, and 22 ms), which are supposed to be remote captures of the response evoked near contact 21 (as shown in Figure 3 D in which the ACEP in ECoG 19, 20, 22 and 23 are equivalent to the ACEP in ECoG 21 up to a scale factor equal to 2.5, 1.3, 1.9 and 4.9 respectively). A double positive potential was also observed, with an early (28.7, 36.4, and 37 ms) but attenuated response and a late component (134.1, 151.6, and 149.7 ms), whose amplitude was also inferior to 300 μ V on contact 6, 5, and 4, respectively.

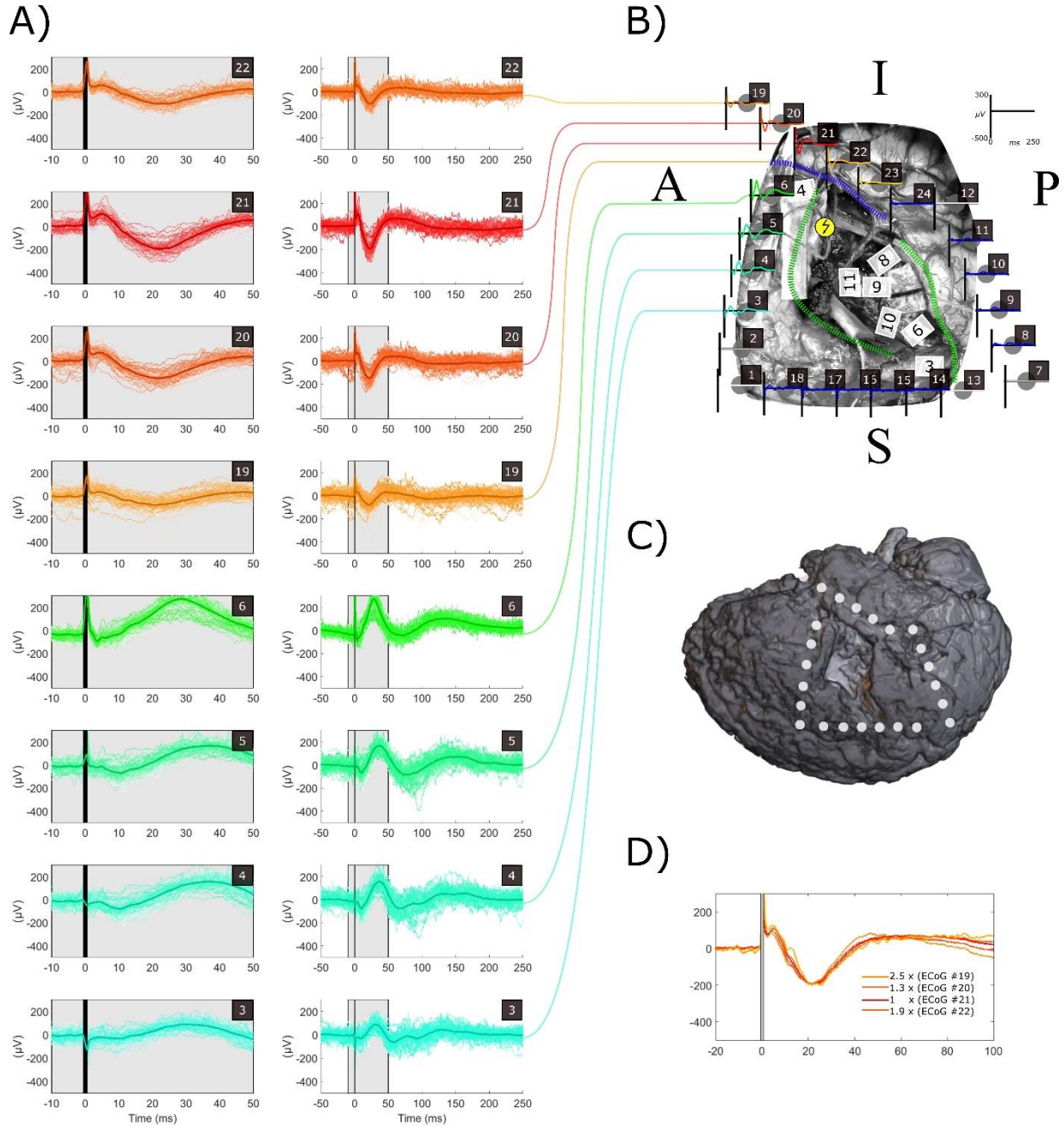


Figure 3. Patient 3: Positioning of ECoG strips (4 x 6 contacts) (B), stimulation sites and ACEP (A and B). 1 x 6 ECoG contacts were placed in posterior part of the medium frontal inferior gyrus (contacts 1-6). The second 1 x 6 ECoG was placed on the supramarginal gyrus (contacts 7-12). Then a third 1x 6 ECoG was placed orthogonally to the central

sulcus (contacts 13-18). And finally the fourth 1 x 6 ECoG was placed in the supratemporal gyrus (contacts 19-24). DES (f=3 Hz, I=2.5 mA, PW=1 ms) was applied subcortically on the white matter pathways on the IFOF, i.e. site 50 (inducing semantic paraphasia during 60 Hz DES mapping). ACEP show different shape and amplitude. Red indicates earlier and greater negative potentials. Green indicates double positive potentials. Blue stand for absence of evoked responses. A) Left signals in the grey box are zoomed from [-10ms; +50ms] in the right column. The black vertical line covers the whole DES artefact. B) The broken arrow in the yellow circle represents the subcortical DES site. Main anatomical landmarks were identified by thick dashed-line: Sylvian fissure in blue, central sulcus in light green, precentral sulcus in dark green. C) Localization of the craniotomy with ECoG positioning in the brain in the 3D post-operative Brain. D) Scaling of ECoG 1, 2, 15 to ECoG 16 in order to illustrate the fact it is roughly the same signal capture remotely on these electrodes.

ACEP: Axono-Cortical Evoked Potentials; DES: Direct Electrical Stimulation; ECoG: ElectroCorticography; IFOF: Inferior Fronto-Occipital Fasciculus.

For Patient 4 (Figure 4), applying DES ($f=3$ Hz, $I=3$ mA, $PW=0.5$ ms) in the resection cavity on the termination of the shortest branch of the arcuate fasciculus induced a main waveform of ACEP. On contact 1, a large negative response (21 ms, $|\text{amplitude}| > 200$ μV) was observed, with an immediate small after-positivity. This response was attenuated on contacts 2, 3, and 4, which were remote captures of the response evoked near contact 1. The amplitude of this negative early potential was very close to, but not greater than, 300 μV , as observed previously for Patients 1 and 2. No very early component occurring before 5 ms was observed for all the responses.

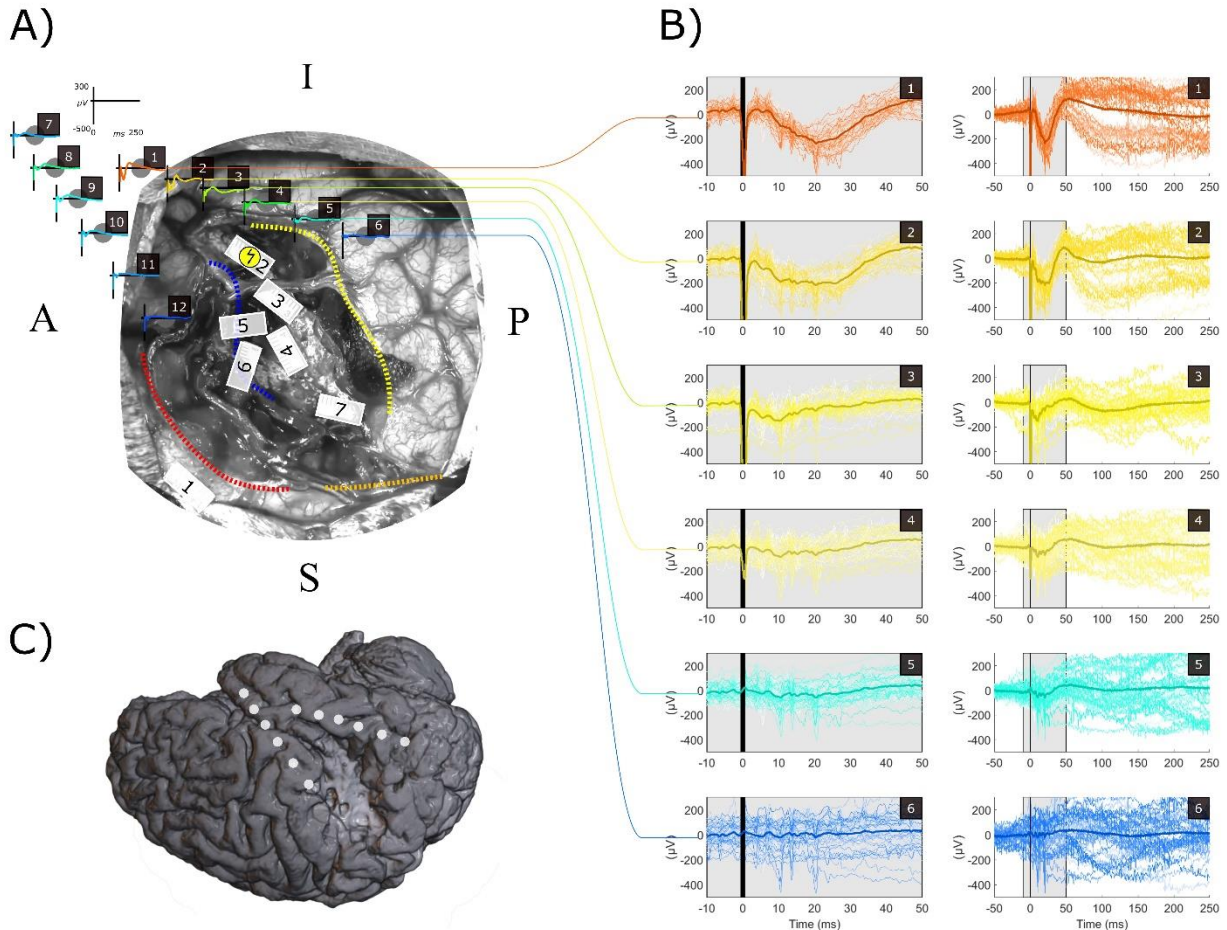


Figure 4. Patient 4: Positioning of ECoG strips (2 x 6 contacts) (B), stimulation sites and ACEP (A and B). The first ECoG strip was located on the posterior part of the superior temporal gyrus. Contact 1 being more anterior part and contact 6 more posterior. The second ECoG strip was located on the posterior part of the inferior frontal gyrus. Contact 7 being more anterior than contact 12. DES ($f=1$ Hz, $I=3$ mA, $PW=0.5$ ms) was applied subcortically on the termination of shortest branch of the arcuate fasciculus, i.e. site 2 (inducing impossibility to perform the 3-digits forward span during 60 Hz DES mapping). ACEP show a main negative monophasic shape. Red indicates earlier and greater negative potentials. Blue stand for absence of evoked responses. A) Left signals in the grey box are zoomed from $[-10\text{ms}; +50\text{ms}]$ in the right column. The black vertical line covers the whole DES artefact. B) The broken arrow in the yellow circle represents the subcortical DES site. Main anatomical landmarks were identified by thick dashed-line: Sylvian fissure in blue, postcentral sulcus in red, temporal superior sulcus in yellow. C) Localization of the craniotomy with ECoG positioning in the brain in the 3D post-operative Brain.

ACEP: Axono-Cortical Evoked Potentials; DES: Direct Electrical Stimulation; ECoG: ElectroCorticography.

For Patient 5 (Figure 5), applying DES ($f=9$ Hz, 2.5 mA, PW=1 ms) in the resection cavity on the frontal aslant tract (FAT) at site 48 induced a main waveform of ACEP. On contacts 15 and 16, a very early negative component (3.1 and 3.1 ms, $|\text{amplitude}| < 100 \mu\text{V}$) was followed by a large positive response (12 and 11.5 ms, $|\text{amplitude}| > 300 \mu\text{V}$), with an immediate small after-negativity. Importantly, the large positive response was the opposite of, and had the same shape as, the early and large negative potential observed in Patients 1-4. Its absolute amplitude was also greater than $300 \mu\text{V}$, as observed previously for Patients 1 and 2. The very early negative component occurring before 5 ms was not observed for contacts 13 and 14.

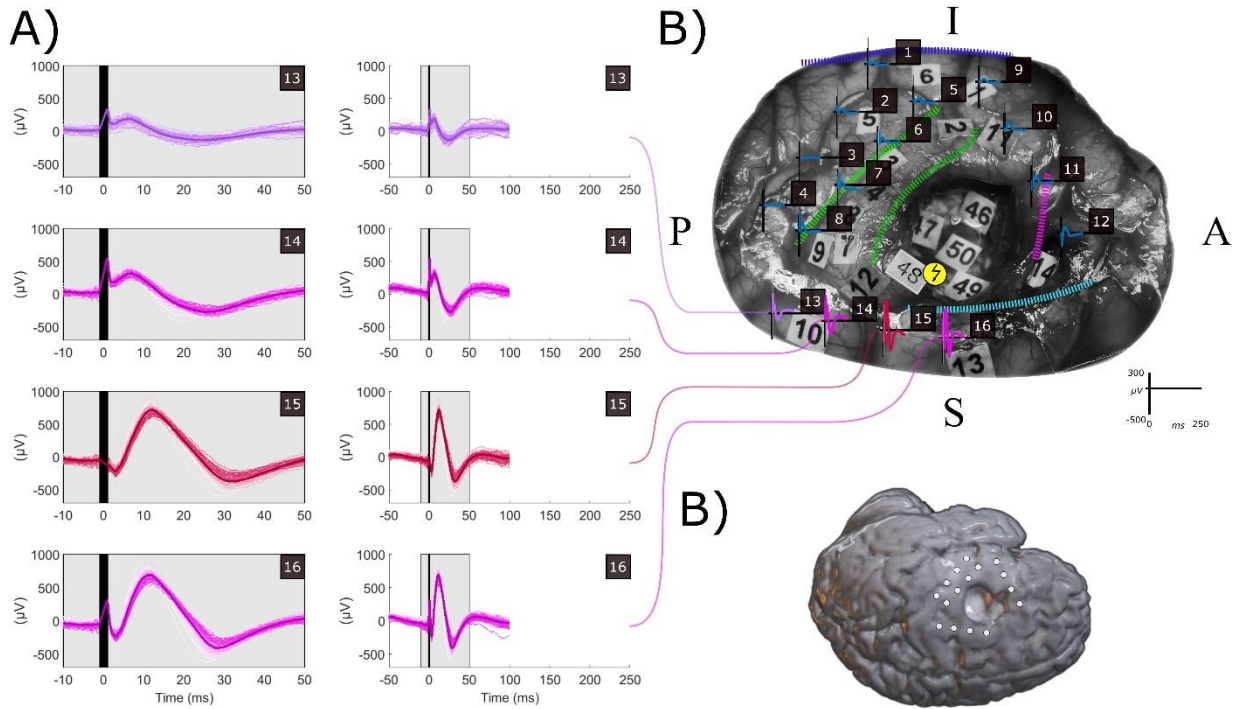


Figure 5. Patient 5: Positioning of ECoG strips (4 x 4 contacts) (B), stimulation sites and ACEP (A and B). (i) The 2 firsts 4 contacts ECoG strips were placed in parallel in pre- (contacts 1 to 4) and post-central (contacts 5 to 8) gyri (1 and 5 being in the more caudal part and 4 and 8 being in the more cranial part); (ii) the third 4 contacts ECoG strips was located in the anterior part of the frontal lobe both in the inferior frontal gyrus (contacts 9 and 10) and in the middle frontal gyrus (contacts 11 and 12); the last and fourth 4 contacts ECoG strips was located in the middle frontal gyrus between the precentral gyrus (contacts 13 and 14) and the premotor cortex (contacts 15 and 16). DES ($f=9$ Hz, $I=2.5$ mA, PW=1 ms) was applied subcortically on the FAT, i.e. site 48 (inducing anarthria during 60 Hz DES mapping). ACEP show a main positive monophasic shape. Red indicates earlier and greater negative potentials. Green indicates double positive potentials. Blue stand for absence of evoked responses. A) Left signals in the grey box are zoomed from [-10ms; +50ms] in the right column. The black vertical line covers the whole DES artefact. Main anatomical landmarks were identified by thick dashed-line: Sylvian fissure in blue, central sulcus in light green, precentral sulcus in dark green, inferior frontal sulcus in cyan, ascendant ramus of the Sylvian fissure in pink. B) The broken arrow in the yellow circle represents the subcortical DES site. C) Localization of the craniotomy with ECoG positioning in the brain in the 3D post-operative Brain.

ACEP: Axono-Cortical Evoked Potentials; DES: Direct Electrical Stimulation; ECoG: ElectroCorticography; FAT: Frontal Aslant Tract.

In Patient 6 (Figure 6), we applied DES to the white matter of the mesial superior frontal gyrus (site 2) using a frequency of 1 Hz, a current of 3 mA, and a pulse width of 0.5 ms. This induced a single waveform of ACEP, which consisted of a double positive potential with an early response (9, 10.6, 11.4 and 16 ms) of attenuated amplitude ($< 200 \mu\text{V}$) and a late response (64, 60, 73 and 95 ms) on contacts 7, 8, 9, and 10 respectively. Interestingly, a slight very early component occurring before 5 ms was observed for contacts 8, 9, and 10. However, the amplitude of this very early component was less than $100 \mu\text{V}$.

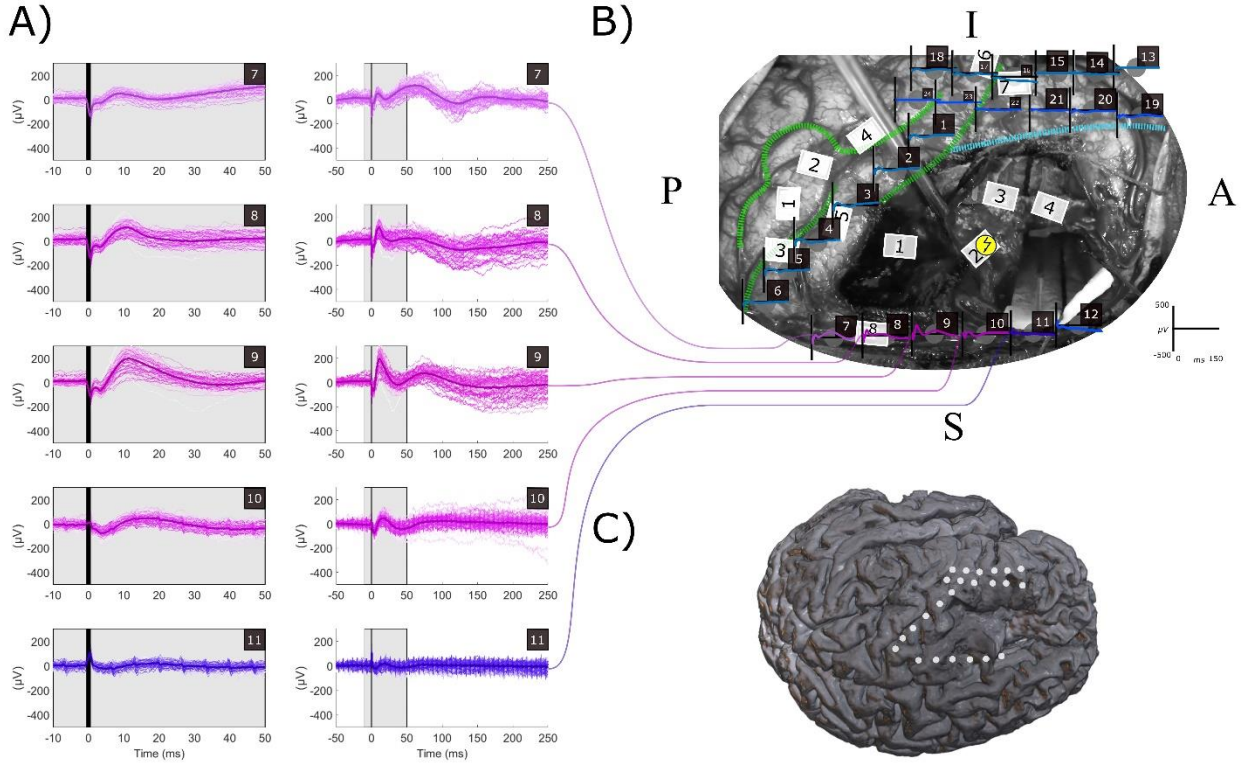


Figure 6. Patient 6: Positioning of ECoG strips (4 x 6 contacts) (A), stimulation sites and ACEP (A and B). (i) The first 6 contact ECoG strips was located in the pre-central gyrus (contacts 1 to 6); (ii) the second 6 contacts ECoG strips was located in the middle frontal gyrus (contacts 7 to 12), (iii) the 2 lasts 6 contacts ECoG strips were placed in the inferior frontal lobe (contacts 13 to 18 being more inferior and contacts 19 to 24 being more superior: 18 and 24 being in the more caudal part and 13 and 19 being in the more cranial part). DES ($f=3\text{Hz}$, $I=3 \text{ mA}$, $PW=0.5 \text{ ms}$) was applied subcortically on the mesial white matter of the superior frontal gyrus, i.e. site 2 (inducing an anomia during 60 Hz DES mapping). ACEP show a double-positive attenuated shape. Green indicates double positive potentials. Blue stand for absence of evoked responses. A) Left signals in the grey box are zoomed from $[-10\text{ms}; +50\text{ms}]$ in the right column. The black vertical line covers the whole DES artefact. Main anatomical landmarks were identified by thick dashed-line: central sulcus in light green, precentral sulcus in dark green, inferior frontal sulcus in cyan. B) The broken arrow in the yellow circle represents the subcortical DES site. C) Localization of the craniotomy with ECoG positioning in the brain in the 3D post-operative Brain.

ACEP: Axono-Cortical Evoked Potentials; DES: Direct Electrical Stimulation; ECoG: ElectroCorticography.

For Patient 7 (Figure 7), we applied DES to the white matter of the superior temporal gyrus using the same parameters as in Patient 6. This induced a single waveform of ACEP, which consisted of a double positive potential with an early response (25 and 25 ms) of attenuated amplitude ($< 200 \mu\text{V}$) and a late response (155 and 155 ms) on contacts 1 and 2 respectively. No very early component occurring before 5 ms was observed for any of the responses.

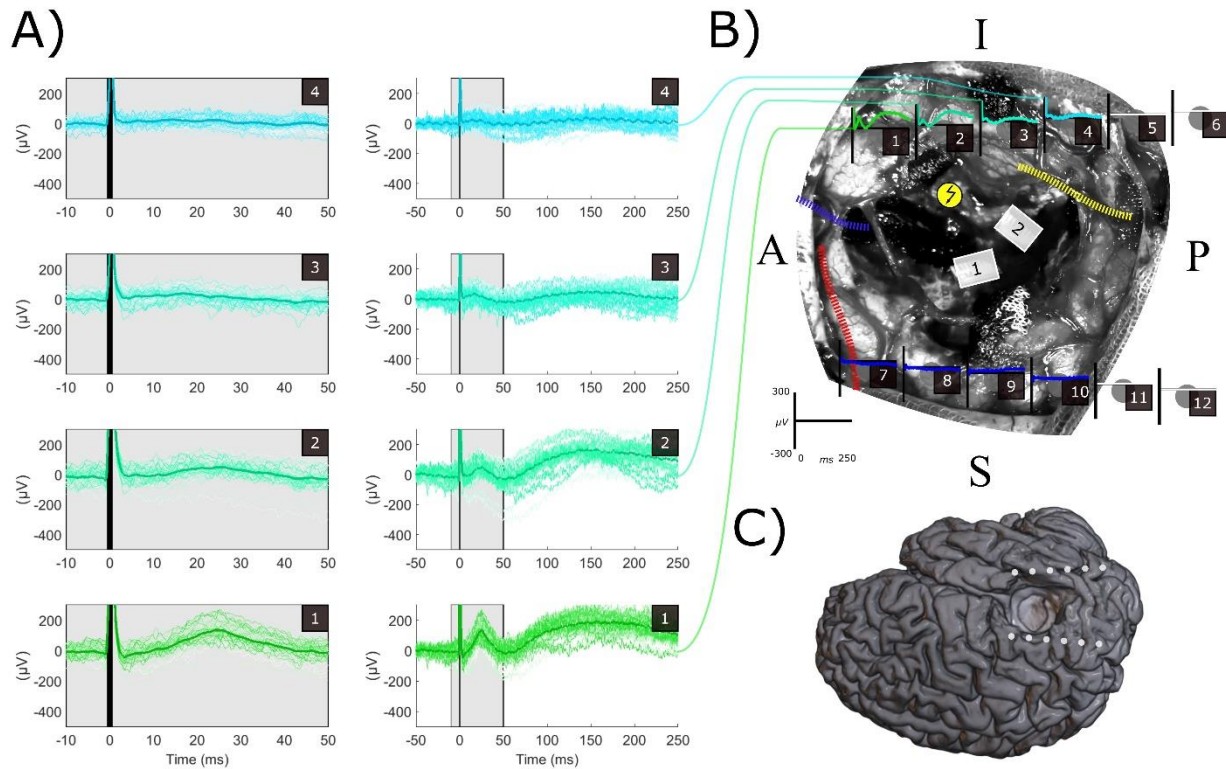


Figure 7. Patient 7: Positioning of ECoG strips (2 x 6 contacts) (B), stimulation sites and ACEP (A and B). (i) The first 6 contacts ECoG strip was placed in the superior temporal gyrus (contacts 1 anterior to 6 posterior); (ii) the second 6 contacts ECoG strips was located in in the pre-central and the post-central gyri (contacts 7 anterior to 12 posterior). DES ($f=1 \text{ Hz}$, $I=3 \text{ mA}$, $PW=0.5 \text{ ms}$) was applied subcortically below ECoG 1. ACEP show double-positive attenuated shape. Green indicates double positive potentials. Blue stand for absence of evoked responses. A) Left signals in the grey box are zoomed from $[-10\text{ms}; +50\text{ms}]$ in the right column. The black vertical line covers the whole DES artefact. B) The broken arrow in the yellow circle represents the subcortical DES site. Main anatomical landmarks were identified by thick dashed-line: Sylvian fissure in blue, post central sulcus in red, temporal superior sulcus in yellow. C) Localization of the craniotomy with ECoG positioning in the brain in the 3D post-operative Brain. ACEP: Axono-Cortical Evoked Potentials; DES: Direct Electrical Stimulation; ECoG: ElectroCorticography.

Discussion

Intraoperative monitoring of brain evoked potentials can potentially determine the connectivity between two sites (stimulation and recording) by electrically stimulating white matter fascicles in the resection cavity and recording the response evoked at the cortical level (ACEP). This is of significant importance for neurosurgery.

In this study, ACEP recordings were conducted on seven patients by stimulating gyral white matter surrounding the surgical cavity immediately after surgical resection. Two types of ACEP waveforms were observed: (1) ACEP with a very early positive peak occurring within the first 5 ms after artifact, followed by a large amplitude early negative component (<40 ms; $|\text{Amplitude}| > 300 \mu\text{V}$), and then a small amplitude after positivity. This waveform was observed in Patients 1-4 with an identical waveform in Patients 5-6 but with polarity inversion. (2) ACEPs with both early (<100 ms) and late (>100 ms) components, both positive with lower amplitudes ($<300 \mu\text{V}$) were observed in Patients 1, 2, 3, and 7. There was no inversion in polarity observed for this second waveform. Importantly, the very early component occurring before 5 ms was not observed in the latter cases. Both types of responses were observed closely in the same patient (one electrode apart), suggesting different electrogenesis.

Regardless of the polarity, the first type of waveform observed in this study resembles the typical pattern seen in DCR and CCEP. It has indeed the characteristics of a DCR (Adrian, 1936; Goldring et al., 1994, 1961; Li and Chou, 1962) *i.e.* composed by a first intense and relatively sharp early negative component called N1, sometimes preceded by a smaller and narrow positive component very close from the stimulation (< 5 ms post-stimulus) and called P0. In DCR and CCEP literature, N1 can be followed by an after positivity or a second late negative component (called N2) occurring for high current stimulation. The very early P0 component strongly suggests that this type of waveform could be a marker of a direct and dense connectivity between stimulation and recording sites. Indeed, P0 has been previously reported for DCR, CCEP and ACEP (Matsumoto et al. 2004, 2007, Yamao et al. 2014, Boyer et al. 2021). P0 may reflect the summation of synchronized action potentials at the level of the somas or axons (Goldring et al., 1994; Landau and Clare, 1956; Stohr et al., 1963; Sugaya et al., 1964). For ACEPs, the size of P0 reflects the connection strength, *i.e.* the number of axons stimulated in the cavity and arriving at the cortical recording site. Moreover, the very short delay (<5 ms) precludes the involvement of any synaptic activities, hence warrants a direct connection between stimulation and recording sites. However, this component is quite difficult to measure properly due to the stimulation artefact and remains much less accessible to on-line thresholding and monitoring for decision making without careful signal processing. It requires a high sampling frequency that few clinical recording systems have.

For CCEP or long-range ACEP, a “propagated P0” was observed and named “P1” by Yamao et al. (2014), to emphasize the conduction delay. In these cases, the electrogenesis is not perfectly clear (by contrast to DCR and short-range ACEP). For a sufficiently dense contingent of AP propagating together on a white matter pathway, a remote summation of AP arriving synchronously at the terminations could be recorded with a delay on the cortical surface. Importantly, in order to testify the recording of the APs synchronized and summed together the P0 or the remote “propagated P0” (P1 in Yamao et al. 2014) should be quite narrow by essence. When too large and too wide, “propagated P0” components should be interpreted with caution as it may not reflect the spatiotemporal summation of short-duration synchronized action potentials but rather

wider electrophysiological events generated at the level of synapses. In such cases, it could also be viewed as a N1 recorded from the other side of the sulcus where it was generated. For the following of this discussion, P1 does not represent the propagated P0 (like in Yamao et al. 2014) but rather the N1 seen from the other side of the sulcus.

In cases where the P0 component cannot be observed, the amplitude of the N1 component (occurring within 40 ms) can serve as a reliable marker of connectivity (Matsumoto et al., 2004, 2007; Boyer et al., 2021). The N1 component is thought to reflect the summation of excitatory post-synaptic potentials (EPSPs) resulting from the activation of different cortical layers (Li and Chou, 1962; Goldring et al., 1994). The greater the amplitude of these early components, the more they suggest a local density of activation from the axonal action potentials that reach the cortical recording site from the white matter stimulated site. This interpretation holds true for patients 5 and 6, even when the polarity of P0 and N1 is reversed to become N0 and P1: the waveforms remain very similar, with only the polarity reversed. This polarity inversion is related to the orientation of the dipole buried within a sulcus and to the placement of the electrodes at the cortical surface on either side of this sulcus, as is well-established for the measurement of somatosensory evoked potentials (Wood et al., 1988). It is worth noting that polarity inversions and N0-P1 sequences are never observed for DCR because the DES and recordings are very close to each other, such that sources are generated at the surface (at the crown of the gyrus) and are not hidden within a sulcus.

In this study, we propose that a P0 (or N0 for Patients 5-6) and an N1 (or P1 for Patients 5-6) waveform thresholded at 100 μ V and 300 μ V, respectively, can be used as discrimination criteria for direct connectivity between the stimulation and recording sites. In situations where the activity around the stimulation site was not simply a passive volume conduction image of it (see patients 1-3 and Figures 1D-3D), we observed a second type of waveform, with a first positive evoked potential of lower amplitude ($< 300 \mu$ V) and sometimes a second positive smooth peak of even weaker amplitude. The electrogenesis of these two positive components remains ambiguous, although they could be considered as the opposite of classical N1 and N2 observed for DCR and ACEP (Adrian, 1936; Goldring et al., 1994, 1961; Li and Chou, 1962). The polarity reversal could correspond to an activity within a sulcus, whose orientation is captured differently depending on the positioning of the surface recording electrode. However, the late component of double positive waveforms, which suggests the involvement of less synchronous polysynaptic circuits, cannot be considered a marker of direct and dense connectivity between the DES site and the recording site. As for the N2 observed in CCEP, the late component of double-positive waveforms suggests, the implication of less synchronous, polysynaptic circuits (locally or distributed over several areas). The N2 being interpreted as the reflection of either the reverberant neuronal activity at the target site or indirect cortico-subcortico-cortical propagation (Matsumoto et al., 2017, 2004). Importantly, the standard N2 peak following the P0/N1 sequence was not observed in the present work, and this may be due to methodological differences in stimulation parameters compared to previous studies on CCEP (Matsumoto et al. 2004, 2007) and ACEP (Yamao et al. 2014). In our study, the stimulation was performed at low intensity ($I < 3$ mA) with a large pulse width ($PW = 0.5-1$ ms) and using a manual bipolar stimulation probe with an inter-electrode distance (IED) of 5mm and 1mm contact diameters (CD). These parameters differ from the ones used for the measurement of CCEP/ACEP in epileptic patients with electrode grids ($I > 8$ mA, $PW = 0.3$ ms, $IED = 1$ cm, $CD = 0.23-0.39$ cm, see (Matsumoto et al., 2012,

2004). These methodological differences might explain why the N2 was not observed (Vincent et al. 2017), although we do not have yet a convincing electrophysiological explanation.

In addition to the possible polarity change discussed earlier, the P1/P2 waveform observed in Patients 1-3 could be attributed to a different type of electrogenesis and/or connectivity processes. There are four hypotheses that could explain this: (i) secondary intracortical spreading after reaching the hot spot, (ii) fan-like divergence of the fascicles towards their cortical termination, which generates several sources, (iii) step by step transmission or rebound through U fibers from the hot spot towards adjacent gyrus, or (iv) connecting different cortical layers, generating excitatory or inhibitory postsynaptic potentials. These four types of evoked activity diffusion are not independent of each other and can coexist.

The hypothesis of secondary intracortical transmission (where the main activity is generated at a cortical site and then spreads around) suggests that the latency of the P1 should increase in accordance with transmission delays. However, we did not observe such delays, making this hypothesis unlikely.

The hypothesis of generating different sources when different branches of the stimulated fascicle reach the cortex prevails when a double positive peak is adjacent to the classical "DCR like" greater response (as seen in contacts 2 and 3 in Patient 1, for example). In this case, both the polarity is reversed and the latency of the N1 or P1 is modified, strongly suggesting another source for the double positive attenuated responses. This multiple source hypothesis could also explain the P1/P2 waveforms observed in Patient 5. In this case, a slight decrease in the latencies of the P1 peaks was observed for contacts 13-14 compared to contacts 15-16, indicating that contact 15-16 captured a common source equidistant to these two contacts but too far from 13-14 to contribute to these contacts, while another source, with faster activation, would be closer to 13-14.

Finally, the possibility of a "rebound" of activity through the U fibers cannot be completely ruled out, but it is unlikely for several reasons. First, if a new volley of action potentials (APs) were triggered from the cortical hot spot towards the adjacent contact, it would result in a delayed P0, which is not observed in any of the patients. Moreover, the amplitude of the P1 observed in some cases is too high to be interpreted as a delayed or propagated P0. Additionally, previous research on micro-stimulation suggests that the activity generated by electrical stimulation is limited to a patch of cortical columns without re-diffusing to the adjacent cortex. For example, a study by Histed et al. (2009) found that as the intensity of the micro-stimulation increased, there was no increase in the stimulated area but an increase in the number of neurons within the same set of cortical columns. Similarly, Logothetis et al. (2010) demonstrated, using micro-stimulation, that only V1 was activated during stimulation of the lateral geniculate nuclei, while V2 and V3 were only activated during the injection of anti-GABAergics, indicating that GABAergic neurons are activated when the external stimulus reaches the target cortex. These findings suggest that local secondary inhibitory activity limits "rebound" phenomena during micro-stimulation, and confines the evoked activity to a well-defined cortical area. However, it remains to be seen whether these observations can be replicated for more meso- or macroscopic activity related to direct electrical stimulation. In the case of DES, the N2 component is often accompanied by a decrease in high gamma activity during its ascending phase (Usami et al., 2015), which likely reflects a summation of inhibitory postsynaptic potentials after the N1 and its associated high gamma activity. This suggests the presence of strong constitutive inhibitory activity aimed at limiting the extension of activity to specific functional compartments within an ensemble of cortical

columns. It is also possible that the after-positivity that occurs just after the N1 with an increase in DES intensity (Goldring et al., 1994) is an example of this initial inhibitory activity aimed at containment.

In conclusion, our study proposes that a recording contact can be classified as a hotspot of direct and dense connectivity to the DES site if its waveform satisfies two criteria: the presence of a small sharp P0/N0 (< 5 ms post stimulus; amplitude > 100 μ V) and a high broader N1/P1 (< 40 ms post stimulus; amplitude > 300 μ V). However, the absence of P0/N0 should not rule out the identification of a hotspot, as it is challenging to measure the earliest response.

Our study has some limitations. First, all stimulation sites were within or close to the white matter of the gyrus, allowing recruitment of all afferent fibers (including association cortico-cortical fibers, callosal fibers and thalamo-cortical fibers). Further investigation is required to determine whether the same results hold for more distant stimulation sites. Secondly, the alignment of axons in the gyral white matter pathways may provide an optimal setting to record ACEPs. However, crossing of multiple pathways in deeper cavities, three-dimensionally more complex (i.e. having more torsion and curvature), may reduce this effect. Additionally, when DES is applied remotely from its cortical output, the evoked responses may be smaller due to the divergence of the tracts (i.e. involving a reduced summation of electrophysiological events, Boyer et al. 2021). Thus, technical limitations of subcortical-cortical distance may exist for recording ACEPs, depending on the stimulation parameters and spatial resolution of the recordings. DES must be sufficiently intense to activate remotely a sufficiently dense contingent of axons allowing the spatiotemporal summation of compact electrophysiological events. Interestingly, however, Yamao et al. 2014 succeeded in recording ACEPs for three patients on the two side of the arcuate fasciculus by stimulating it in its middle but with different DES settings than ours.

Lastly, our interpretations were qualitative and based on simplified electrogenesis models, such as the dipole model. Although widely used in electrophysiology, the dipole model constitutes an extreme simplification of underlying phenomena (Buzsáki et al., 2012). Thus, further biophysical modeling or experimental measurements, such as current source density (Ness et al., 2020), are necessary to advance these interpretations. Better identification of hotspots of direct connectivity could be obtained by solving the inverse problem with source localization algorithms. Exploring the cortical surface with multiple measures is crucial for this purpose.

Funding

Research supported by French “Association pour la Recherche sur le Cancer” (ARC-France, project n° ARCPGA12019110000940_1572), the LabEx NUMEV project (n° ANR- 10-LABX-0020) within the I-Site MUSE (ANR-16-IDEX-0006); and INRIA through an associate team between France (FB) and Japan (RM). RM was supported by a Kobe University Strategic International Collaborative Research Grant (Type B Fostering Joint Research) between Japan (RM) and France (HD, FB), and JSPS KAKENHI 22H02945, 22H04777.

Conflict of interest

None of the authors have potential conflicts of interest to be disclosed.

References

- Adrian ED. The spread of activity in the cerebral cortex. *J Physiol* 1936;88:127–61. <https://doi.org/10.1113/jphysiol.1936.sp003427>.
- Aubrun S, Poisson I, Barberis M, Draou C, Toure M, Madadaki C, et al. The challenge of overcoming the language barrier for brain tumor awake surgery in migrants: a feasibility study in five patient cases. *Acta Neurochir (Wien)* 2020;162:389–95. <https://doi.org/10.1007/s00701-019-04101-1>.
- Boyer A, Duffau H, Mandonnet E, Vincent M, Ramdani S, Guiraud D, et al. Attenuation and Delay of Remote Potentials Evoked by Direct Electrical Stimulation During Brain Surgery. *Brain Topogr* 2020;33:143–8. <https://doi.org/10.1007/s10548-019-00732-w>.
- Boyer A, Duffau H, Vincent M, Ramdani S, Mandonnet E, Guiraud D, et al. Electrophysiological Activity Evoked by Direct Electrical Stimulation of the Human Brain: Interest of the P0 Component. 2018 40th Annu. Int. Conf. IEEE Eng. Med. Biol. Soc., IEEE; 2018, p. 2210–3. <https://doi.org/10.1109/EMBC.2018.8512733>.
- Boyer A, Ramdani S, Duffau H, Dali M, Vincent M. Electrophysiological Mapping During Brain Tumor Surgery: Recording Cortical Potentials Evoked Locally, Subcortically and Remotely by Electrical Stimulation to Assess the Brain Connectivity On-line. *Brain Topogr* 2021a;34:221–33. <https://doi.org/10.1007/s10548-020-00814-0>.
- Boyer A, Stengel C, Bonnetblanc F, Dali M, Duffau H, Rheault F, et al. Patterns of axono-cortical evoked potentials: an electrophysiological signature unique to each white matter functional site? *Acta Neurochir (Wien)* 2021b;163:3121–30. <https://doi.org/10.1007/s00701-020-04656-4>.
- Buzsáki G, Anastassiou CA, Koch C. The origin of extracellular fields and currents — EEG, ECoG, LFP and spikes. *Nat Rev Neurosci* 2012;13:407–20. <https://doi.org/10.1038/nrn3241>.
- Chang H-T. Dendritic potential of cortical neurons produced by direct electrical stimulation of the cerebral cortex. *J Neurophysiol* 1951;14:1–21. <https://doi.org/10.1152/jn.1951.14.1.1>.
- Deras P, Moulinié G, Maldonado IL, Moritz-Gasser S, Duffau H, Bertram L. Intermittent General Anesthesia With Controlled Ventilation for Asleep-Awake-Asleep Brain Surgery. *Neurosurgery* 2012;71:764–72. <https://doi.org/10.1227/NEU.0b013e3182647ab8>.
- Duffau H. Stimulation mapping of white matter tracts to study brain functional connectivity. *Nat Rev Neurol* 2015;11:255–65. <https://doi.org/10.1038/nrneurol.2015.51>.
- Eccles JC. Interpretation of action potentials evoked in the cerebral cortex. *Electroencephalogr Clin Neurophysiol* 1951;3:449–64. [https://doi.org/10.1016/0013-4694\(51\)90033-8](https://doi.org/10.1016/0013-4694(51)90033-8).
- Enatsu R, Gonzalez-Martinez J, Bulacio J, Mosher JC, Burgess RC, Najm I, et al. Connectivity of the frontal and anterior insular network: A cortico-cortical evoked potential study. *J Neurosurg* 2016;125:90–101. <https://doi.org/10.3171/2015.6.JNS15622>.
- Enatsu R, Matsumoto R, Piao Z, O'Connor T, Horning K, Burgess RC, et al. Cortical negative motor network in comparison with sensorimotor network: A cortico-cortical evoked potential study. *Cortex* 2013;49:2080–96. <https://doi.org/10.1016/j.cortex.2012.08.026>.
- Goldring S, Harding GW, Gregorie EM. Distinctive electrophysiological characteristics of functionally discrete brain areas: a tenable approach to functional localization. *J Neurosurg* 1994;80:701–9. <https://doi.org/10.3171/jns.1994.80.4.0701>.
- Goldring S, JERVA MJ, HOLMES TG, O'LEARY JL, SHIELDS JR. Direct Response of Human

Cerebral Cortex. Arch Neurol 1961;4:590–8. <https://doi.org/10.1001/archneur.1961.00450120004002>.

Histed MH, Bonin V, Reid RC. Direct Activation of Sparse, Distributed Populations of Cortical Neurons by Electrical Microstimulation. Neuron 2009;63:508–22. <https://doi.org/10.1016/j.neuron.2009.07.016>.

Landau WM, Clare MH. A note on the characteristic response pattern in primary sensory projection cortex of the cat following a synchronous afferent volley. Electroencephalogr Clin Neurophysiol 1956;8:457–64. [https://doi.org/10.1016/0013-4694\(56\)90011-6](https://doi.org/10.1016/0013-4694(56)90011-6).

Li C-L, Chou SN. Cortical intracellular synaptic potentials and direct cortical stimulation. J Cell Comp Physiol 1962;60:1–16. <https://doi.org/10.1002/jcp.1030600102>.

Logothetis NK, Augath M, Murayama Y, Rauch A, Sultan F, Goense J, et al. The effects of electrical microstimulation on cortical signal propagation. Nat Neurosci 2010;13:1283–91. <https://doi.org/10.1038/nn.2631>.

Mandonnet E, Dadoun Y, Poisson I, Madadaki C, Froelich S, Lozeron P. Axono-cortical evoked potentials: A proof-of-concept study. Neurochirurgie 2016;62:67–71. <https://doi.org/10.1016/j.neuchi.2015.09.003>.

Mandonnet E, Winkler PA, Duffau H. Direct electrical stimulation as an input gate into brain functional networks: principles, advantages and limitations. Acta Neurochir (Wien) 2010;152:185–93. <https://doi.org/10.1007/s00701-009-0469-0>.

Matsumoto R, Kunieda T, Nair D. Single pulse electrical stimulation to probe functional and pathological connectivity in epilepsy. Seizure 2017;44:27–36. <https://doi.org/10.1016/j.seizure.2016.11.003>.

Matsumoto R, Nair DR, Ikeda A, Fumuro T, Lapresto E, Mikuni N, et al. Parieto-frontal network in humans studied by cortico-cortical evoked potential. Hum Brain Mapp 2012;33:2856–72. <https://doi.org/10.1002/hbm.21407>.

Matsumoto R, Nair DR, LaPresto E, Bingaman W, Shibasaki H, Luders HO. Functional connectivity in human cortical motor system: a cortico-cortical evoked potential study. Brain 2006;130:181–97. <https://doi.org/10.1093/brain/awl257>.

Matsumoto R, Nair DR, LaPresto E, Najm I, Bingaman W, Shibasaki H, et al. Functional connectivity in the human language system: A cortico-cortical evoked potential study. Brain 2004;127:2316–30. <https://doi.org/10.1093/brain/awh246>.

Miller KJ, Müller K, Hermes D. Basis profile curve identification to understand electrical stimulation effects in human brain networks. PLoS Comput Biol 2021;17:e1008710. <https://doi.org/10.1371/journal.pcbi.1008710>.

Ness T V., Haldnes G, Næss S, Pettersen KH, Einevoll GT. Computing extracellular electric potentials from neuronal simulations. Adv. Exp. Med. Biol., 2020, p. 179–99. <https://doi.org/https://doi.org/10.48550/arXiv.2006.16630>.

Stohr PE, Goldring S, O’Leary JL. Patterns of unit discharge associated with direct cortical response in monkey and cat. Electroencephalogr Clin Neurophysiol 1963;15:882–8. [https://doi.org/10.1016/0013-4694\(63\)90177-9](https://doi.org/10.1016/0013-4694(63)90177-9).

Sugaya E, Goldring S, O’Leary JL. Intracellular potentials associated with direct cortical response and seizure discharge in cat. Electroencephalogr Clin Neurophysiol 1964;17:661–9. [https://doi.org/10.1016/0013-4694\(64\)90234-2](https://doi.org/10.1016/0013-4694(64)90234-2).

Usami K, Matsumoto R, Kobayashi K, Hitomi T, Shimotake A, Kikuchi T, et al. Sleep modulates cortical connectivity and excitability in humans: Direct evidence from neural activity induced by single-pulse electrical stimulation. *Hum Brain Mapp* 2015;36:4714–29. <https://doi.org/10.1002/hbm.22948>.

Vincent M, Guiraud D, Duffau H, Mandonnet E, Bonnetblanc F. Electrophysiological brain mapping: Basics of recording evoked potentials induced by electrical stimulation and its physiological spreading in the human brain. *Clin Neurophysiol* 2017;128:1886–90. <https://doi.org/10.1016/j.clinph.2017.07.402>.

Vincent M, Rossel O, Hayashibe M, Herbet G, Duffau H, Guiraud D, et al. The difference between electrical microstimulation and direct electrical stimulation – towards new opportunities for innovative functional brain mapping? *Rev Neurosci* 2016;27:231–58. <https://doi.org/10.1515/revneuro-2015-0029>.

Vincent MA, Bonnetblanc F, Mandonnet E, Boyer A, Duffau H, Guiraud D. Measuring the electrophysiological effects of direct electrical stimulation after awake brain surgery. *J Neural Eng* 2020;17:016047. <https://doi.org/10.1088/1741-2552/ab5cdd>.

Wasserman D, Valero-Cabré A, Dali M, Stengel C, Boyer A, Rheault F, et al. Axono-cortical evoked potentials as a new method of IONM for preserving the motor control network: a first study in three cases. *Acta Neurochir (Wien)* 2021;163:919–35. <https://doi.org/10.1007/s00701-020-04636-8>.

Wood CC, Spencer DD, Allison T, McCarthy G, Williamson PD, Goff WR. Localization of human sensorimotor cortex during surgery by cortical surface recording of somatosensory evoked potentials. *J Neurosurg* 1988;68:99–111. <https://doi.org/10.3171/jns.1988.68.1.0099>.

Yamao Y, Matsumoto R, Kunieda T, Arakawa Y, Kobayashi K, Usami K, et al. Intraoperative dorsal language network mapping by using single-pulse electrical stimulation. *Hum Brain Mapp* 2014;35:4345–61. <https://doi.org/10.1002/hbm.22479>.